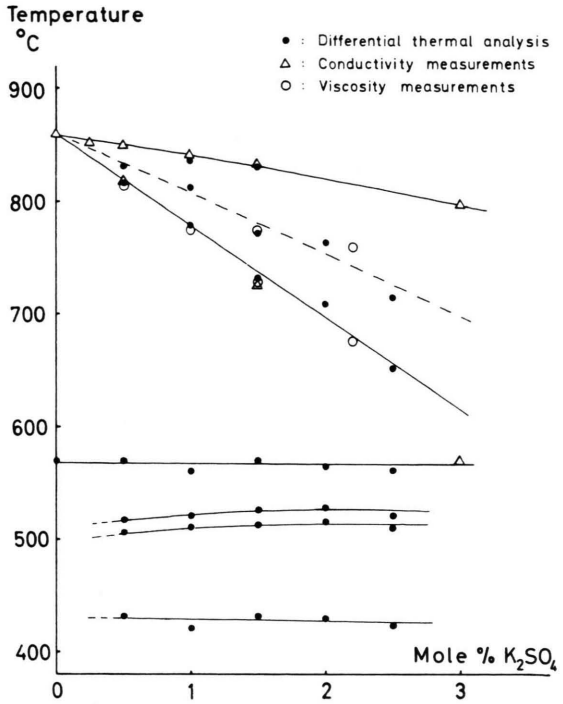

structural changes might be due to the rotation properties of the sulphate ions, which should cause only small changes in the conductivity.

The decrease in $\varkappa$ and increase in η when less than about 1.2 mole% K_2SO_4 is added can be explained by assuming that a small amount of potassium ions can be accomodated in the octahedral positions of the sulphate lattice [6, 11]. At higher concentration of potassium ions there is probably a formation of dislocations.

A further discussion of the different phases must wait until X-ray investigations have been performed.

This work was financially supported by the Swedish Technical Research Council.

Fig. 5. The phase diagram of Li_2SO_4 with small quantities of K_2SO_4.

Refractive Index Measurements of Molten Salts with Wave-front-shearing Interferometry

I. Test of Apparatus and Procedure

LENNART W. WENDELÖV, LARS-ERIK WALLIN, and SILAS E. GUSTAFSSON

Institutionen för Fysik, Chalmers Tekniska Högskola, Göteborg

(Z. Naturforschg. **22 a**, 1180—1184 [1967]; received 21 April 1967)

A wave-front-shearing interferometer has been used for refractive index measurements on liquids. A test series on water gave agreement within $\pm 5 \cdot 10^{-5}$ with earlier data. The refractive index of molten potassium nitrate has been measured between 340 and 460 °C and found to depend linearly on temperature according to the equation

$$n = 1.46478 - 1.579 \cdot 10^{-4} \cdot t$$

at a wavelength of 6330 Å.

I. General Description of the Method

An interferometer with two SAVART plates has previously been used more or less as a refractive index recording instrument [1]. In the present work it is used as a path difference measuring device by utilization of the wellknown technique of rotating a plane parallel glass plate in the light path. The two vertically sheared, partially overlapping wave-fronts interfere to give three sets of straight, vertical fringes in the plane where the glass plate immersed in the liquid is imaged. The upper and lower parts of the image consist of light passing only through glass or through liquid, respectively, giving rise to non-moving fringes. In the middle portion, of height equal to the shear distance and representing the vicinity of the edge of the glass plate, the fringes are the result of interference of light passing through glass with light passing through liquid. The position of these fringes is a measure of the path difference

[1] O. BRYNGDAHL and S. LJUNGGREN, J. Phys. Chem. **64**, 1264 [1960].

between the two beams. Thus the fringes will move as the glass plate is rotated around a vertical axis. By determination of the position of the fringes for a certain rotation of the glass plate, or (which amounts to the same thing and being the only feasible method with the large path differences used in practice) by counting the number of fringes passing a fixed point in the image, the path difference can be calculated from the formula [2]

$$\Delta Z = h[\,(n^2 - n_v^2 \sin^2\alpha)^{1/2} - n + n_v(1-\cos\alpha)\,] \quad (1)$$

where h = thickness of the glass plate, n = refractive index of the glass plate, n_v = refractive index of the liquid, α = angle of rotation.

The present technique was developed in order to get a simple and accurate method for the determination of the refractive index of molten salts. The SAVART interferometer has certain advantages for this purpose: 1. The liquid can be contained in one single cell of relatively small dimensions and the apertures of the furnace can be kept small and at fixed positions. This facilitates the thermostating problems, which are generally difficult in accurate high temperature work. 2. The interferometer provides automatically the reference system necessary for the observation of the fringe movement, and it is not necessary to work with polychromatic light and to keep track of any achromatic fringe [3].

II. Experimental Setup

The interferometer as described in ref. [1] had to be modified to a certain extent for the following reasons.

The visibility of the fringes is equal to the absolute value of the degree of coherence for quasi-monochromatic light [4a]. In the normal use of the interferometer, only the space coherence [5] needs to be considered, the shear distance setting a limit to the source slit width to be used [6], while the generally moderate path differences do not give any problems with time coherence. In the present case the importance of the latter is evident from the fact that no fringes at all can be seen in the middle section if a high pressure mercury arc is used as light source. With a low pressure arc, however, the visibility of the fringes is excellent when the glass plate is perpendicular to the direction of the light.

According to the VAN CITTERT–ZERNICKE theorem the degree of coherence $|\mu_{12}|$ between the vibrations at two points P_1 and P_2 in the object plane and thus the visibility V of the fringes in the image plane, are determined by [4b]

$$V = |\mu_{12}| \approx \frac{\sin(\pi\, p\, l'/\lambda)}{\pi\, p\, l'/\lambda} \cdot \frac{\sin(\pi\, q\, h'/\lambda)}{\pi\, q\, h'/\lambda}$$

for quasi-monochromatic light. Here l' and h' are the horizontal and vertical dimensions of the source slit and p und q are essentially the horizontal and vertical angular distances between P_1 and P_2 as seen from the center of the source slit. h' has to be kept small since the nature of the technique requires a rather large shear distance; thus l' must be large because of intensity considerations. This means that even a very small sidewise shift of the beam when passing the rotated glass plate is sufficient to decrease the visibility of the fringes considerably. In practice it turns out that a sufficient number of fringes cannot by far be counted before the fringes vanish completely.

In the first effort to overcome this problem the light beam was allowed to pass a second glass plate, identical to the first one and rotated the same angle in the opposite direction. Thus the beam was restored to its original horizontal coordinate. The arrangement was successful from the optical point of view, but the experimental procedure involving the turning of the glass plates and measuring the angles made it less attractive.

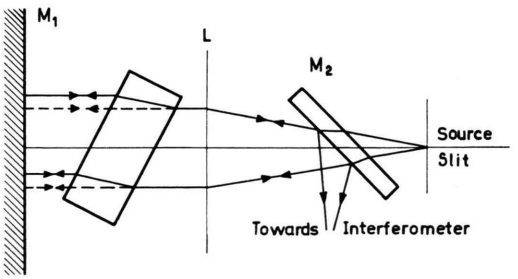

Fig. 1. Experimental setup.

[2] L. H. ADAMS, J. Wash. Acad. Sci. **8**, 265 [1915].
[3] cf. ADAMS [2].
[4] M. BORN and E. WOLF, Principles of Optics, Pergamon Press, 3rd ed., London 1965. a) p. 506; b) p. 510, Eq. (26); p. 393, Eq. (1).
[5] For terminology see e.g. E. WOLF, Opt. Acta **13**, 281 [1966].
[6] O. BRYNGDAHL, Arkiv Fysik **21**, 334 [1961].

The final arrangement is shown in Fig. 1. A mirror M_1, adjusted to make the image of the source slit coincide with the slit, reflects the light back through the optical system. Another mirror M_2, partially transmittant, sends part of the reflected light into the interferometer. The lens L thus acts both as the collimator lens and as the first member of the demagnifying system. The broken lines indicate the path of the light passing only through the liquid and below the glass plate. (The cell containing the liquid is not shown in the figure.)

The glass plate is attached to a vertical axis which can be turned by means of a horizontal lever of length l. The movement of the latter can be measured to within $\pm 1\,\mu$ by means of a gauge. The necessary readings are:

1. The position of the lever when perpendicular to the line of motion of the gauge arm: reading s_0.
2. The position of the lever when the glass plate is perpendicular to the light beam: reading s_1. s_0 and s_1 are approximately equal.
3. The position of the lever after counting a certain number of fringes: reading s_2.

The angle of rotation α of the glass plate is determined (apart from a small correction due to the specific mechanical construction of our apparatus) from the expression

$$\alpha = \arctan[(s_2 - s_0)/l] - \arctan[(s_1 - s_0)/l]. \quad (2)$$

The refractive index n_v of the liquid is obtained from Eq. (1)

$$n_v = \tfrac{1}{2} n \left\{ T_1 + 1 + \left[1 - (T_1^2 + 2T_1) \frac{1+\cos\alpha}{1-\cos\alpha} \right]^{1/2} \right\} \quad (3)$$

where $T_1 = m\lambda/(2hn)$, m = number of fringes; the glass thickness is taken as $2h$ since the light passes twice through the plate.

Also the refractive index n of the glass plate may be calculated if that of the surrounding medium is known

$$n = n_v \left[1 + T_2 \frac{\frac{1}{2} T_2 + \cos\alpha}{1 - \cos\alpha - T_2} \right] \quad (4)$$

where $T_2 = m\lambda/(2hn_v)$.

The refractive indices used are referred to air of ambient temperature (dry air, 760 mm Hg, 0.03% CO_2). Thus the wave length to be used is the air wave length; its dependence on temperature (t, °C) is allowed for by the formula

$$\lambda_t = (n_{15}/n_t) \cdot \lambda_{15}, \qquad \lambda_{15} = 5\,460.724\ \text{Å}. \quad (5)$$

The refractive index n_t of air is computed from Eq. (6), which is a consequence of the LORENTZ–LORENZ law

$$n_t = n_{15} - (n_{15} - 1)\,\gamma(t - 15),$$
$$n_{15} = 1.0002772, \qquad \gamma = 0.003685\ \text{deg.}^{-1} \quad (6)$$

III. Experiments

I. Two series of test experiments were made:

1. The refractive index of the glass plate (vitreous quartz) was determined by rotating the plate in air. The results are shown in Table 1.

2. The refractive index of water was determined at various temperatures, the index of quartz being taken as $n = 1.46015 + 1.1 \cdot 10^{-5}\ (t - 20)$ [7]. Measurements were made for several angles of rotation, ranging from approximately 10 to 25 degrees for each temperature. The consistency of the values for different angles was good. In Table 2 only the maximum rotations are shown together with the corresponding number of fringes counted. The refractive indices given are the averages for the different se-

$t = 20.00$ °C			$t = 32.80$ °C		
α°	m	n	α°	m	n
12.5246	278,53	1.46010	12,5125	278.04	1.46024
14.9228	397.06	1.46014	14.9125	396.54	1.46021
17.2678	534.20	1.46018	17.2595	533.71	1.46022
19.5536	688.58	1.46015	19.5483	688.20	1.46016
21.7756	858.88	1.46015	21.7730	858.76	1.46023
Average value		1.46014	Average value		1.46019
Literature value[7]		1.46015	Literature value[7]		1.46029

Table 1. Refractive index of vitreous quartz relative to air for $\lambda = 5461$ Å.

[7] LANDOLT-BÖRNSTEIN, Zahlenwerte und Funktionen, 6th ed., vol. II.

t °C	$\alpha°$	m	n_v average of series	Max. dev.	n_v literature[7]
20.03	21.7841	320.50	1.33443	$2 \cdot 10^{-5}$	1.33445
22.30	24.1970	401.25	1.33417	$2 \cdot 10^{-5}$	1.33422
24.75	24.1610	400.56	1.33399	$3 \cdot 10^{-5}$	1.33398
30.00	21.7633	322.66	1.33337	$5 \cdot 10^{-5}$	1.33340
36.72	21.7733	325.13	1.33246	$2 \cdot 10^{-5}$	1.33246
40.03	21.7733	326.43	1.33195	$5 \cdot 10^{-5}$	1.33196

Table 2. Refractive index of water relative to air for $\lambda = 5461$ A.

ries. The fifts column gives the maximum deviations from the mean value.

II. A determination of the refractive index of molten potassium nitrate[8] as a function of temperature is shown in Table 3. The data were fitted to the least squares equation

$$n_v = n_0 - b\,t, \qquad 340\,°\mathrm{C} < t < 460\,°\mathrm{C},$$

with $n_0 = 1.46478 \pm 0.00012$

and $b = (1.579 \pm 0.003) \cdot 10^{-4}\ \mathrm{deg.}^{-1}$,

t, °C	$\lambda = 5461$ Å[9]	$\lambda = 5893$ Å[10]	$\lambda = 6330$ Å[8]
341.7	1.420	1.415	1.41088
348.9	1.419	1.414	1.40974
369.6	1.415	1.410	1.40639
402.6	1.410	1.405	1.40120
410.0	1.409	1.403	1.40001
429.8	1.406	1.400	1.39696
456.7	1.401	1.395	1.39273

Table 3. Refractive index of molten potassium nitrate relative to vacuum.

where the probable errors are given. A slight nonlinear temperature dependence of refractive index is responsible for the somewhat larger errors in this case. For these measurements a laser was available ($\lambda = 6330$ Å) which removed the problems of coherence mentioned above. For comparison two sets of older measurements are shown.

IV. Estimation of Errors and Discussion

The following expressions for the errors are derived from Eq. (3):

$$\Delta n_v = \left| T_1 \frac{\partial n_v}{\partial T_1} \right| \left(\left| \frac{\Delta m}{m} \right| + \left| \frac{\Delta \lambda}{\lambda} \right| + \left| \frac{\Delta h}{h} \right| \right) + \left| \left(n_v - T_1 \frac{\partial n_v}{\partial T_1} \right) \frac{\Delta n}{n} \right| + \left| \alpha \frac{\partial n_v}{\partial \alpha} \frac{\Delta \alpha}{\alpha} \right| . \qquad (7)$$

One obtains a similar expression for Δn from Eq. (4) just by substituting n for n_v and T_2 for T_1 in the preceding equation. It turns out that the coefficients for the relative errors are approximately constant. The error of the angle of rotation, derived from Eq. (2) becomes

$$\Delta\alpha = l^{-1}(|\Delta s_0| \sin^2\alpha + |\Delta s_1| + |\Delta s_2| \cos^2\alpha + \tfrac{1}{2}|\Delta l| \sin^2 2\alpha). \qquad (8)$$

The estimated errors are as follows: $|\Delta s_0| = |\Delta s_2| = 10^{-3}$ mm, $|\Delta s_1| = 2 \cdot 10^{-3}$ mm, $|\Delta l| = 5 \cdot 10^{-3}$ mm, $|\Delta m| = 2 \cdot 10^{-2}$, $|\Delta h| = 10^{-4}$ mm, $|\Delta\lambda| \approx 0$, $|\Delta n| = 10^{-5}$, $|\Delta n_v| \equiv 0$ (for air). Introduction of the appropriate values in the equations gives

$$|\Delta n_v| = 5 \cdot 10^{-5} \text{ for water,}$$

$$|\Delta n_v| = 5 \cdot 10^{-5} \text{ for } KNO_3,$$

and $$|\Delta n| = 2 \cdot 10^{-4} \text{ for quartz.}$$

Two sources of systematic errors should be considered:

1. If the condition $\tau \ll (\Delta\nu)^{-1}$, ($\tau = \Delta Z/c$, $\Delta Z =$ path difference, $c =$ velocity of light, $\Delta\nu =$ frequency width of the spectral line) is not fulfilled, the fringes are shifted[4a] compared to the position in ideally monochromatic light, the shift being dependent on τ. In principle this would mean that the shift is not constant during an experiment. In order to find out the "quality" of the light from the mercury lamp, a simple semiquantitative experiment was made: A number of glass plates were stacked in the light path and the fringes in the shear area were observed. The path difference corresponding to vanishing visibility was approximately 12 mm, indicating that the change of the path difference during an experiment (400 fringes $\approx$ 0.2 mm) should have little influence on the position of the fringes.

[8] These measurements are described in more detail elsewhere: L. W. Wendelöv, S. E. Gustafsson, N.-O. Halling, and R. A. E. Kjellander, to be published.

[9] J. Zarzycki and F. Naudin, C. R. Acad. Sci. Paris **256**, 1282 [1963].

[10] H. Bloom and D. C. Rhodes, J. Phys. Chem. **60**, 791 [1956].

2. Dissolved air in the liquid should have an influence on the refractive index. The change of the index by saturation with carbon dioxide [11] of atmospheric pressure is $-3 \cdot 10^{-5}$. Since the solubility of this gas is approximately 50 times as large as that of air, it may be assumed that this error is much less than other errors involved [12].

As can be seen from the error calculations the accuracy is not comparable to available precision techniques at room temperature, however, it should be possible to increase the accuracy considerably by using an improved device for the determination of the angles of rotation and by an increase of the thickness of the glass plate giving a larger number of fringes.

Acknowledgement: This investigation is supported by the Swedish Technical Research Counsil.

[11] International Critical Tables VII, p. 13.
[12] L. W. Tilton and J. K. Taylor, J. Res. Nat. Bur. Stand. **20**, 419 [1938]; RP 1085.

Untersuchung des Elektrotransportes in der β-Phase des Systems Nickel–Antimon

Th. Heumann und H. Stüer

Institut für Metallforschung der Universität Münster i. W.

(Z. Naturforschg. **22 a**, 1184—1189 [1967]; eingegangen am 3. April 1967)

In der β-Phase mit der Zusammensetzung $Ni_{0,717}Sb_{0,283}$, die der Gruppe der β–Hume–Rothery-Phasen zuzuordnen ist, wurde der durch Gleichstrom verursachte Materietransport untersucht. Nur Nickel wird transportiert und zwar zur Anode. Gemäß der durch strukturelle Leerstellen bedingten hohen Beweglichkeit der Nickel-Atome ist der Effekt auch bei kleinen Stromdichten erstaunlich groß. Die Auswertung der Ergebnisse nach der Theorie von Fiks bzw. Huntington steht nicht im Widerspruch zu der Hume–Rothery-Regel, nach welcher die Elektronenkonzentration 1,5 betragen sollte und Nickel als nullwertig anzusehen ist.

Die Untersuchung des durch Gleichstrom bewirkten Materietransports in Metallen und Legierungen, des sogen. Elektrotransports, ist geeignet, uns wertvolle Informationen über die elektronischen, atomaren und strukturellen Eigenschaften sowie über Bindungsverhältnisse zu liefern. Soweit sich diese Informationen auf qualitative Schlußfolgerungen beziehen, steht heute fest, daß in der oben genannten Stoffklasse der Transport überwiegend durch eine Wechselwirkung der Ladungsträger mit den für Platzwechsel befähigten Metallatomen oder besser positiven Ionen zustande kommt. In vielen Fällen ist die normale Feldkraft, die in Ionenleitern die entscheidende Rolle spielt, hier vernachlässigbar klein gegenüber der durch Impulsübertragung verursachten Mitführkraft. Wenn auch die qualitativen Angaben bereits wertvolle Erkenntnisse geben, so ist es doch unerläßlich, quantitative Zusammenhänge herzustellen. In dieser Hinsicht sind zwei wichtige Bedingungen zu erfüllen. Die erste Forderung ist, daß die Meßergebnisse den Grad von Genauigkeit besitzen, der erforderlich ist, um quantitative Schlüsse ziehen zu können. Zum anderen muß die Theorie des Elektrotransports genügend gesichert sein. Bedauerlicherweise reicht die bis heute erreichte Meßgenauigkeit nicht aus, zu entscheiden, welche von den zur Zeit diskutierten Theorien die richtige ist. Auch die vorliegende Arbeit, die zwar den Vorteil bietet, daß der Transporteffekt ungewöhnlich groß ist, kann keine Entscheidung treffen.

Theoretische Zusammenhänge

Als Transportzahl τ_i definiert man die Anzahl der Mole der Komponente i, die pro Sekunde und pro Ampere relativ zum Gitter der betreffenden Probe transportiert wird:

$$\tau_i = n_i / I\,t\,, \tag{1}$$

n_i ist die während der Versuchszeit t durch den Strom I überführte Molmenge.

Andererseits läßt sich die Zahl der Mole n_i, die infolge einer auf die Teilchen der Komponente i wirkenden Kraft K_i transportiert wird, berechnen. Es gilt:

$$n_i = B_i \cdot K_i \cdot q\,t\,\gamma_i / V\,, \tag{2}$$

wo B_i eine Beweglichkeit, q der Querschnitt der Probe, γ_i der Molenbruch und V das Molvolumen